

# Sudden change of geometric quantum discord in finite temperature reservoirs

Ming-Liang Hu\* and Jian Sun

*School of Science, Xi'an University of Posts and Telecommunications, Xi'an 710061, China*

We investigate sudden change (SC) behaviors of the distance-based measures of geometric quantum discords (GQDs) for two non-interacting qubits subject to the two-sided and the one-sided thermal reservoirs. We found that the GQDs defined by different distances exhibit different SCs, and thus the SCs are the combined result of the chosen discord measure and the property of a state. We also found that the thermal reservoir may generate states having different orderings related to different GQDs. These inherent differences of the GQDs reveal that they are incompatible in characterizing quantum correlations both quantitatively and qualitatively.

PACS numbers: 03.65.Ud, 03.65.Ta, 03.67.Mn

Key Words: Geometric quantum discord; Trace distance; Bures distance; Hellinger distance

## I. INTRODUCTION

Due to the emergence of quantum information science, the characterization and quantification of quantum correlations in a system have become one of the people's research focuses in the past few decades [1]. Nowadays, when we mention to quantum correlations, two prominent lines of research on this problem may immediately appear in our minds. The first one centers around the entanglement-separability paradigm, under which various forms of the entanglement measures have been proposed and extensively studied [2]. The second one is based on the noncommutativity of operators in quantum mechanics, and along this line people also presented a plenty of discord-like quantum correlation measures [3].

It is well accepted that entanglement is responsible for the advantage of many quantum communication and computation tasks [4–6]. It is also realized recently that quantum discord [7], which reveals quantum correlations from a different perspective, plays a vital role in quantum protocols such as the deterministic quantum computation with one qubit [8], remote state preparation [9], quantum locking of classical correlations [10, 11], quantum state broadcasting [12], and quantum state merging [13, 14]. Moreover, the discord consumption has been linked to the quantum advantage for extracting information via coherent interactions [15], and meanwhile, it can also be connected to entanglement via some measurement processes [16].

Although both can serve as physical resources for quantum information processing, quantum discord and entanglement are in fact fundamentally different in many aspects. The most prominent one is that quantum discord may be increased by local operations [17], while entanglement can only be increased by coherent operations. Moreover, when considering their evolution for open quantum system, quantum discord and entanglement also exhibit distinct singular behaviors. For instance, quantum discord is more robust against decoherence than entanglement [18–20], it is immune to certain quantum noises during certain time intervals [21–25], and therefore exhibits the frozen behavior which is impossible for entangle-

ment. Quantum discord exhibits sudden changes (SCs) due to the optimization procedure involved in its definition [26–32], while entanglement undergoes sudden death [33] which does not exist for quantum discord. It is also worthwhile to note that the sudden death of entanglement is independent of the chosen entanglement measures, as it occurs whenever the evolved state becomes separable.

We investigate in this work the singular behaviors of three kinds of the geometric quantum discords (GQDs) for two non-interacting qubits subjecting to the independent thermal reservoirs. We will show that for both the two-sided and the one-sided reservoirs, there are SCs being observed during the evolution of the GQDs, and the critical times for their occurrence are strongly dependent on the choice of the discord measures, which means that this phenomenon is the combined result of the chosen discord measure and the quantum state other than a property of the state itself. This statement is further confirmed by the relativity of different GQDs, i.e., different GQDs may impose different orderings of quantum states.

We arrange this paper as follows. In Sections II and III, we recall the formula for the three GQDs, and present the analytical solution for the master equation describing the evolution of the system. Then in Section IV, we give a discussion of the SC phenomenon. Finally, Section V is devoted to a summary.

## II. DISTANCED-BASED MEASURES OF THE GQDS

As we mentioned in Section I, the quantum discord in a system can be quantified from different perspectives. We adopt in this work three forms of the distance-based measures of GQDs [34–42]. They are defined via the minimal distance from  $\rho$  to  $\Omega_0$ , i.e.,

$$D_\alpha(\rho) = \min_{\chi \in \Omega_0} d_\alpha(\rho, \chi) \quad (1)$$

where  $d_\alpha$  designates the different distance measures one used in defining the GQDs. They are all well defined and can avoid the problem for the GQD based on the Frobenius norm [43]. We concentrate in the following on a bipartite system  $AB$  described by the density operator  $\rho$ , and the three GQDs are defined respectively via the trace distance [34–37], the Hellinger distance [38, 39], and the Bures distance [40–42]. To facilitate

---

\*Electronic address: mingliang0301@163.com

later description, we call them the TDD, HDD, and BDD for brevity.

We first recall the corresponding measures for the trace distance, the Hellinger distance, and the Bures distance between  $\rho$  and  $\chi$ , which are given respectively by

$$\begin{aligned} d_T(\rho, \chi) &= \|\rho - \chi\|_1, \\ d_H(\rho, \chi) &= \|\sqrt{\rho} - \sqrt{\chi}\|_2, \\ d_B(\rho, \chi) &= [2(1 - \sqrt{F(\rho, \chi)})]^{1/2}, \end{aligned} \quad (2)$$

where  $\|\cdot\|_1$  and  $\|\cdot\|_2$  denote respectively the trace norm and the Frobenius norm, while  $F(\rho, \chi) = [\text{tr}(\sqrt{\rho\chi\rho})^{1/2}]^2$  represents the Uhlmann fidelity.

Then, the TDD, HDD, and BDD can be defined respectively via the minimal  $d_T(\rho, \chi)$ ,  $d_H(\rho, \chi)$ , and  $d_B(\rho, \chi)$  as

$$\begin{aligned} D_T(\rho) &= \min_{\chi \in \Omega_0} \|\rho - \chi\|_1, \\ D_H(\rho) &= 2 \min_{\sqrt{\chi} \in \Omega'_0} \|\sqrt{\rho} - \sqrt{\chi}\|_2^2, \\ D_B(\rho) &= \sqrt{(2 + \sqrt{2}) \min_{\chi \in \Omega_0} (1 - \sqrt{F(\rho, \chi)})}, \end{aligned} \quad (3)$$

where the set  $\Omega_0$  is usually taken to be the classical-quantum state  $\Omega_0 = \sum_k (\Pi_k^A \otimes I_B) \rho (\Pi_k^A \otimes I_B)$ , and  $\Omega'_0 = \sum_k (\Pi_k^A \otimes I_B) \sqrt{\rho} (\Pi_k^A \otimes I_B)$ , with  $\{\Pi_k^A\}$  being the projection-valued measurements. Moreover, the constants 2 and  $2 + \sqrt{2}$  before min are introduced for the normalization of  $D_H(\rho)$  and  $D_B(\rho)$  for the two-qubit maximally discordant states.

The calculation of the TDD, HDD, and BDD is a hard task for general  $\rho$ , and analytical results exist only for certain special classes of states. First, for the two-qubit  $X$  state  $\rho^X$  which only contains nonzero elements along the main diagonal and anti-diagonal, the TDD is given by [37]

$$D_T(\rho^X) = \sqrt{\frac{\xi_1^2 \xi_{\max} - \xi_2^2 \xi_{\min}}{\xi_{\max} - \xi_{\min} + \xi_1^2 - \xi_2^2}}, \quad (4)$$

where  $\xi_{1,2} = 2(|\rho_{23}| \pm |\rho_{14}|)$ ,  $\xi_3 = 1 - 2(\rho_{22} + \rho_{33})$ ,  $\xi_{\max} = \max\{\xi_3^2, \xi_2^2 + x_{A3}^2\}$ , and  $\xi_{\min} = \min\{\xi_1^2, \xi_3^2\}$ , with  $x_{A3} = 2(\rho_{11} + \rho_{22}) - 1$ .

Second, for the  $2 \times n$  dimensional state  $\rho$ , and the decomposed  $\sqrt{\rho} = \sum_{ij} c_{ij} X_i \otimes Y_j$ , with  $\{X_i : i = 0, 1, 2, 3\}$  and  $\{Y_j : j = 0, 1, \dots, n^2 - 1\}$  constituting the orthonormal operator bases for the Hilbert spaces  $\mathcal{H}_A$  and  $\mathcal{H}_B$ , the HDD can be calculated as [38]

$$D_H(\rho) = 2(1 - \|\mathbf{r}\|_2^2 - z_{\max}), \quad (5)$$

where  $\|\mathbf{r}\|_2^2 = \sum_j c_{0j}^2$ , and  $z_{\max}$  represents the largest eigenvalue of the matrix  $ZZ^\dagger$ , with  $Z = (c_{ij})_{i=1,2,3;j=0,1,\dots,n^2-1}$ .

Finally, although there is no analytic solution, the calculation for the maximum of  $F(\rho, \chi)$  can be simplified as [42]

$$F_{\max}(\rho, \chi) = \frac{1}{2} \max_{\|\vec{u}=1\|} \left( 1 - \text{tr} \Lambda + 2 \sum_{k=1}^n \lambda_k(\Lambda) \right), \quad (6)$$

where  $\lambda_k(\Lambda)$  denote the eigenvalues of  $\Lambda = \sqrt{\rho}(\vec{u} \cdot \vec{\sigma} \otimes I_B) \sqrt{\rho}$  in non-increasing order, with  $\vec{u}$  being a unit vector in  $\mathbb{R}^3$ , and  $\vec{\sigma} = (\sigma^x, \sigma^y, \sigma^z)$  is the vector of the Pauli operators.

From the above equations, one can note that even for the simple  $X$  state, there are optimization procedures involved for obtaining the GQDs, and this may induce SC behaviors of  $D_\alpha(\rho)$ . We will discuss them explicitly in the following text.

### III. SOLUTIONS OF THE MODEL

The central system we considered consists of two qubits (labeled as  $S = A, B$ ) with large enough spatial distance, and the direct interaction between them can be ignored. We will discuss two different cases: (i) both qubits  $A$  and  $B$  are embedded in their own independent thermal reservoirs, and (ii) only qubit  $A$  (or  $B$ ) is embedded in the thermal reservoir, while the other one is free of noise.

For the qubit  $S$  subject to the thermal reservoir, the evolution of  $\rho^S(t)$  is governed by the master equation [44]

$$\frac{d\rho^S}{dt} = \frac{\gamma_S}{2} \sum_{k=1}^2 \left( 2\mathcal{L}_k^S \rho^S \mathcal{L}_k^{S\dagger} - \{L_k^{S\dagger} \mathcal{L}_k^S, \rho^S\} \right), \quad (7)$$

under the Markovian approximation. Here,  $\gamma_S$  is the strength of the damping rate,  $\{\cdot, \cdot\}$  denotes the anticommutator, while  $\mathcal{L}_1^S = \sqrt{\bar{n} + 1} \sigma_S^-$  and  $\mathcal{L}_2^S = \sqrt{\bar{n}} \sigma_S^+$  (with  $\sigma_S^\pm$  being the raising and the lowering operators) describe, respectively, the decay and excitation processes of the qubit  $S$ , with rates depending on the temperature which is proportional to the average thermal photons  $\bar{n}$  in the reservoir.

The master equation (7) can be solved analytically. For convenience of later presentation, we define

$$q_1^S = \frac{\bar{n} + (\bar{n} + 1)p_S^2}{2\bar{n} + 1}, \quad q_2^S = \frac{\bar{n}(1 - p_S^2)}{2\bar{n} + 1}, \quad (8)$$

then one can obtain that  $\rho^S(t)$  takes the following form

$$\rho^S(t) = \begin{pmatrix} q_1^S \rho_{11}^S(0) + q_2^S \rho_{00}^S(0) & p_S \rho_{10}^S(0) \\ p_S \rho_{01}^S(0) & 1 - q_1^S \rho_{11}^S(0) - q_2^S \rho_{00}^S(0) \end{pmatrix}, \quad (9)$$

where  $\rho_{ij}^S = \langle i | \rho^S | j \rangle$  in the standard basis  $\{|1\rangle, |0\rangle\}$  expanded

by the eigenvectors of the Pauli operator  $\sigma_S^z$ , and the time-

dependent factor  $p_S = e^{-(2\bar{n}+1)\gamma_S t/2}$ . Moreover, when  $\bar{n} = 0$ , the reservoir is at zero temperature, and the solution of Eq. (9) reduces to that given in Ref. [45].

From the analytical expression for the single-qubit reduced density matrix  $\rho^S(t)$ , one can obtain the two-qubit density matrix  $\rho(t)$  for arbitrary initial state  $\rho(0)$  by using the procedure presented in Ref. [45]. The diagonal elements are given by

$$\begin{aligned}\rho_{11}(t) &= q_1^A q_1^B \rho_{11}(0) + q_1^A q_2^B \rho_{22}(0) + q_2^A q_1^B \rho_{33}(0) \\ &\quad + q_2^A q_2^B \rho_{44}(0), \\ \rho_{22}(t) &= q_1^A [(1 - q_1^B) \rho_{11}(0) + (1 - q_2^B) \rho_{22}(0)] \\ &\quad + q_2^A [(1 - q_1^B) \rho_{33}(0) + (1 - q_2^B) \rho_{44}(0)], \\ \rho_{33}(t) &= (1 - q_1^A) [q_1^B \rho_{11}(0) + q_2^B \rho_{22}(0)] \\ &\quad + (1 - q_2^A) [q_1^B \rho_{33}(0) + q_2^B \rho_{44}(0)], \\ \rho_{44}(t) &= 1 - \rho_{11}(t) - \rho_{22}(t) - \rho_{33}(t),\end{aligned}\quad (10)$$

while the nondiagonal elements are given by

$$\begin{aligned}\rho_{12}(t) &= q_1^A p_B \rho_{12}(0) + q_2^A p_B \rho_{34}(0), \\ \rho_{13}(t) &= q_1^B p_A \rho_{13}(0) + q_2^B p_A \rho_{24}(0), \\ \rho_{14}(t) &= p_A p_B \rho_{14}(0), \quad \rho_{23}(t) = p_A p_B \rho_{23}(0), \\ \rho_{24}(t) &= p_A (1 - q_1^B) \rho_{13}(0) + p_A (1 - q_2^B) \rho_{24}(0), \\ \rho_{34}(t) &= (1 - q_1^A) p_B \rho_{12}(0) + (1 - q_2^A) p_B \rho_{34}(0),\end{aligned}\quad (11)$$

and the other nondiagonal elements can be written directly by using the Hermitian condition  $\rho_{ij}(t) = \rho_{ji}^*(t)$ .

For the special case of  $p_A = p_B = p$ , we obtain the two-sided identical reservoir  $\mathcal{E}_{AB} = \mathcal{E}_A \otimes \mathcal{E}_B$ , while for  $p_A = p$  and  $p_B = 1$  ( $p_A = 1$  and  $p_B = p$ ), it reduces to the one-sided reservoir  $\mathcal{E}_A$  ( $\mathcal{E}_B$ ).

#### IV. SC OF THE GQDS

Based on the solutions in Eqs. (10) and (11) for the system-reservoir coupling mode presented in Section III, we begin to discuss decay dynamics of the three GQDs. We will show that they exhibit distinct singular behaviors, which include the completely different SCs and their relativity on characterizing quantum correlations. To be explicit, we consider initial two-qubit state of the following form

$$|\Psi\rangle = \alpha|11\rangle + \beta|00\rangle, \quad (12)$$

where  $\alpha \in [0, 1]$ , and  $\beta = \sqrt{1 - \alpha^2}$ . The analytical expressions of  $\rho(t)$  for both the two-sided identical reservoirs  $\mathcal{E}_{AB}$  and the one-sided reservoir  $\mathcal{E}_A$  (or  $\mathcal{E}_B$ ) can be written directly from Eqs. (10) and (11), which are of the  $X$  form.

We first consider the two-sided identical reservoir  $\mathcal{E}_{AB}$ . Fig. 1 is an exemplified plot of the  $\gamma t$  dependence of  $D_T(\rho)$ ,  $D_B(\rho)$ , and  $D_H(\rho)$  for the initial state  $|\Psi\rangle$  with  $\bar{n} = 0.6$  and different values of  $\alpha^2$ . For this case, as  $\rho_{23}(t) = 0$ , the TDD can be obtained analytically as

$$D_T(\rho) = 2p^2\alpha\sqrt{1 - \alpha^2}, \quad (13)$$

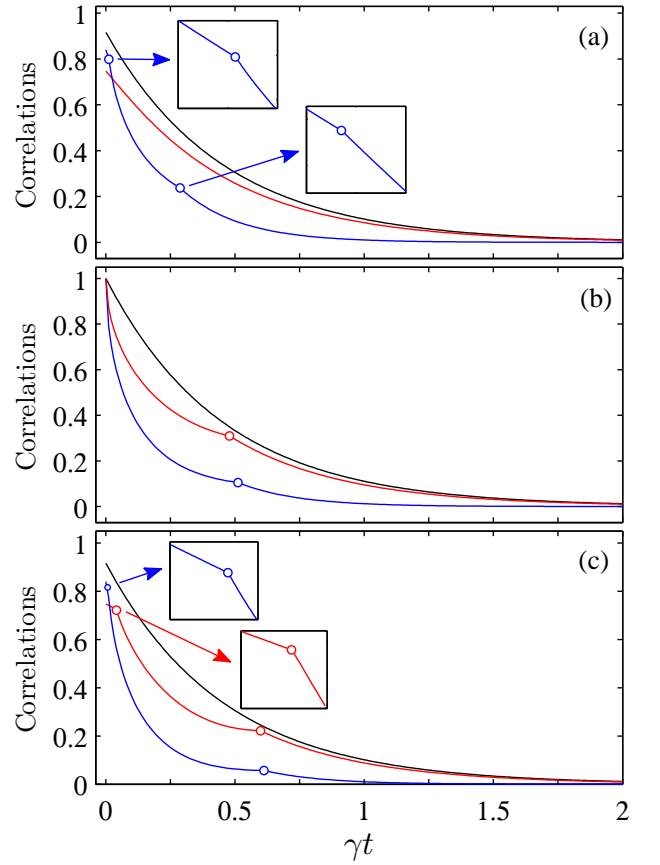


FIG. 1: (Color online)  $\gamma t$  dependence of  $D_T(\rho)$  (black),  $D_B(\rho)$  (red), and  $D_H(\rho)$  (blue) for the initial state  $|\Psi\rangle$  subject to the two-sided reservoir  $\mathcal{E}_{AB}$  with  $\bar{n} = 0.6$ . The other parameters are given by  $\alpha^2 = 0.3$  (a), 0.5 (b), and 0.7 (c). The hollow circles denote the SC points.

therefore it is symmetric with respect to  $\alpha^2 = 0.5$ , and decays smoothly and monotonously with increasing  $\gamma t$  for any  $\alpha^2$ .

The BDD and the HDD are no longer the symmetric functions of  $\alpha^2 = 0.5$ . As displayed in Fig. 1, while both  $D_B(\rho)$  and  $D_H(\rho)$  still decay monotonously with increasing  $\gamma t$ , there are also SCs being observed, i.e., they are nonsmooth functions of  $\gamma t$ . In particular, the critical time  $\gamma t_c$  for the SCs and the times of SCs are determined strongly by the chosen discord measure and the form of the initial state. For the chosen parameters in Fig. 1,  $D_B(\rho)$  decays smoothly for  $\alpha^2 = 0.3$ , while  $D_H(\rho)$  experiences double SCs at  $\gamma t_c \simeq 0.0115$  and  $0.287$ , respectively. For  $\alpha^2 = 0.5$ , the single SC of  $D_B(\rho)$  ( $\gamma t_c \simeq 0.478$ ) occurs earlier than that of  $D_H(\rho)$  ( $\gamma t_c \simeq 0.5115$ ), while for  $\alpha^2 = 0.7$ , both  $D_B(\rho)$  and  $D_H(\rho)$  exhibit double SCs, where the first one of  $D_B(\rho)$  ( $\gamma t_c \simeq 0.0404$ ) occurs shortly after  $D_H(\rho)$  ( $\gamma t_c \simeq 0.0066$ ), and the second one of  $D_B(\rho)$  ( $\gamma t_c \simeq 0.5985$ ) turns out to be a little bit earlier than that of  $D_H(\rho)$  ( $\gamma t_c \simeq 0.6113$ ).

Next we turn to discuss the cases of the one-sided reservoirs  $\mathcal{E}_A$  and  $\mathcal{E}_B$ . We displayed in Fig. 2 the  $\gamma t$  dependence of the GQDs by the solid and the dash-dotted lines, respectively. As for these two cases, only one of the two qubits is exposed to

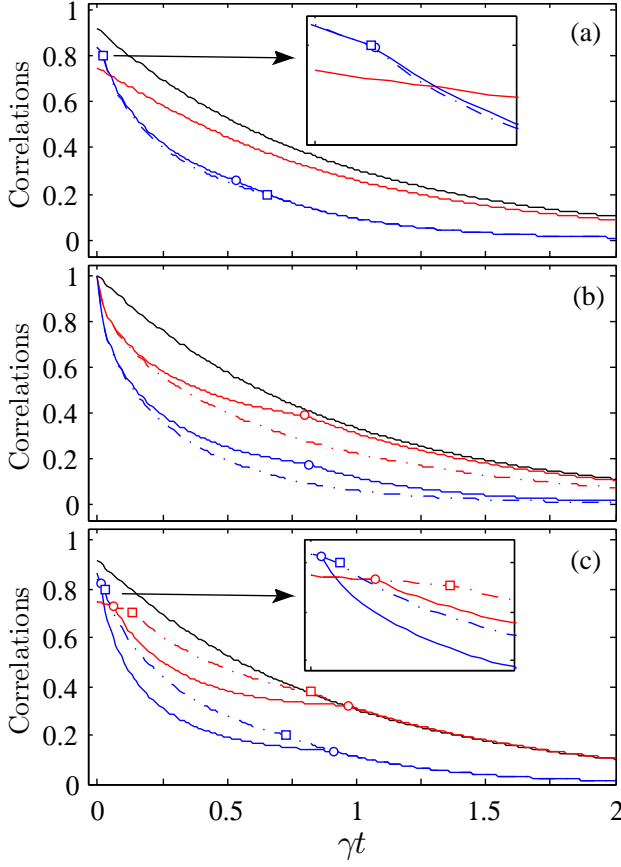


FIG. 2: (Color online)  $\gamma t$  dependence of  $D_T(\rho)$  (black),  $D_B(\rho)$  (red), and  $D_H(\rho)$  (blue) for the initial state  $|\Psi\rangle$  subject to the one-sided reservoir  $\mathcal{E}_A$  (solid) or  $\mathcal{E}_B$  (dash-dotted) with  $\bar{n} = 0.6$ . The other parameters are  $\alpha^2 = 0.3$  (a),  $0.5$  (b), and  $0.7$  (c). The hollow circles and squares denote the SC points. Moreover, the lines of  $D_T(\rho)$ , as well as the lines of  $D_B(\rho)$  with  $\alpha^2 = 0.3$ , are overlapped for the  $\mathcal{E}_A$  and  $\mathcal{E}_B$  cases.

the reservoir, the decay of the GQDs is slower than that for the two-sided reservoir case. First, for both  $\mathcal{E}_A$  and  $\mathcal{E}_B$ , the TDD is always given by

$$D_T(\rho) = 2p\alpha\sqrt{1-\alpha^2}, \quad (14)$$

which is still a symmetric function about  $\alpha^2 = 0.5$ , and decays smoothly and monotonously with the increasing  $\gamma t$ .

The BDD and the HDD may do not behave as smooth functions of  $\gamma t$ . For the one-sided reservoir  $\mathcal{E}_A$ , they exhibit qualitatively the same behaviors as those for the  $\mathcal{E}_{AB}$  case, and the only difference is that the critical times for the SCs are all obviously delayed. For  $\alpha^2 = 0.3$ , the double SCs for  $D_H(\rho)$  occur at  $\gamma t_c \simeq 0.024$  and  $0.536$ , respectively. For  $\alpha^2 = 0.5$ , the single SC for  $D_B(\rho)$  and  $D_H(\rho)$  occurs respectively at  $\gamma t_c \simeq 0.802$  and  $0.816$ . Finally, for  $\alpha^2 = 0.7$ , the double SCs for  $D_B(\rho)$  occur at  $\gamma t_c \simeq 0.0611$  and  $0.966$ , while for  $D_H(\rho)$  they occur at  $\gamma t_c \simeq 0.01045$  and  $0.914$ .

For the one-sided reservoir  $\mathcal{E}_B$ , although the evolved density matrix differs only in  $\rho_{22}(t)$  and  $\rho_{33}(t)$  from the  $\mathcal{E}_A$  case, the BDD and HDD are not exactly the same (cf. the solid and

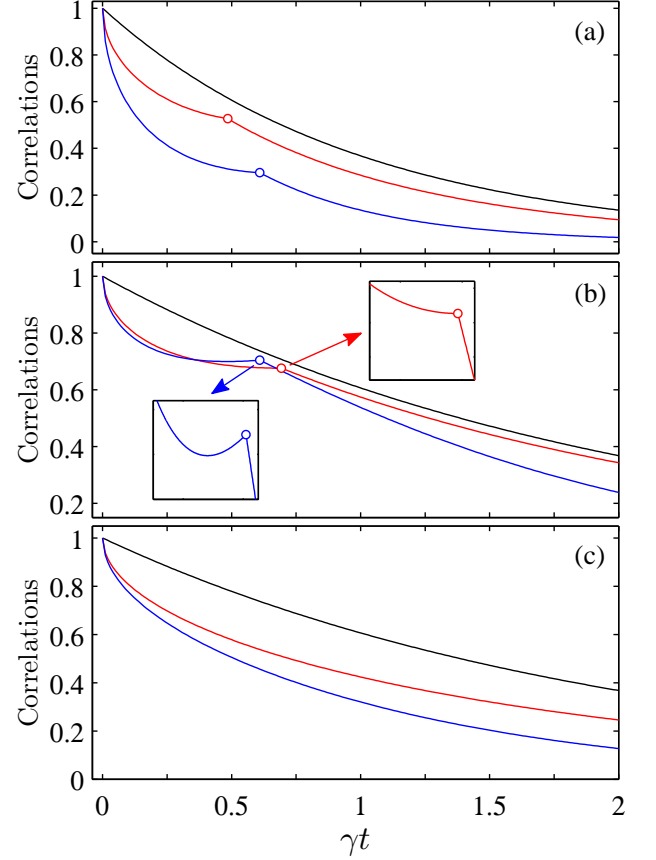


FIG. 3: (Color online)  $\gamma t$  dependence of  $D_T(\rho)$  (black),  $D_B(\rho)$  (red), and  $D_H(\rho)$  (blue) for the initial state  $|\Psi\rangle$  subject to the two-sided reservoirs  $\mathcal{E}_{AB}$  (a), one-sided reservoir  $\mathcal{E}_A$  (b), and  $\mathcal{E}_B$  (c), all with the parameters  $\bar{n} = 0$  and  $\alpha^2 = 0.5$ . The hollow circles denote the SC points.

the dash-dotted lines in Fig. 2). For  $\alpha^2 = 0.3$ ,  $D_B(\rho)$  exhibits completely the same  $\gamma t$  dependence compared with that of the  $\mathcal{E}_A$  case, while the double SCs of  $D_H(\rho)$  ( $\gamma t_c \simeq 0.022$  and  $0.652$ ) are slightly different. Moreover, the single SC for both  $D_B(\rho)$  and  $D_H(\rho)$  disappears for  $\alpha^2 = 0.5$ . Finally, for  $\alpha^2 = 0.7$ , the first SC of  $D_B(\rho)$  ( $\gamma t_c \simeq 0.1305$ ) and  $D_H(\rho)$  ( $\gamma t_c \simeq 0.027$ ) occurs later than that of the  $\mathcal{E}_A$  case, while their second SC ( $\gamma t_c \simeq 0.822$  and  $0.724$ , respectively) occurs earlier than that of the  $\mathcal{E}_A$  case.

The decay rates of the GQDs for  $\mathcal{E}_A$  and  $\mathcal{E}_B$  may also be different. As showed in Fig. 2, for  $\alpha^2 = 0.5$ ,  $D_B(\rho)$  and  $D_H(\rho)$  for the  $\mathcal{E}_B$  case decay faster than those for the  $\mathcal{E}_A$  case in the whole  $\gamma t$  region. For  $\alpha^2 = 0.3$  and  $0.7$ , however,  $\mathcal{E}_A$  and  $\mathcal{E}_B$  give different decay rates of  $D_B(\rho)$  and  $D_H(\rho)$  only during limited  $\gamma t$  regions. For  $\alpha^2 = 0.3$ ,  $D_H(\rho)$  for the  $\mathcal{E}_B$  case decays slightly faster than that for the  $\mathcal{E}_A$  case when  $\gamma t \in [0.022, 0.652]$ , while for  $\alpha^2 = 0.7$ ,  $D_B(\rho)$  and  $D_H(\rho)$  for the  $\mathcal{E}_B$  case decay slower than those for the  $\mathcal{E}_A$  case when  $\gamma t \in [0.0611, 0.966]$  and  $\gamma t \in [0.01045, 0.914]$ , respectively.

We discussed in the above evolution of the three GQDs, and observed distinct singular behaviors such as the single and the double SCs caused exclusively by the reservoir. We discuss

in the following two limiting cases, i.e., the zero temperature ( $\bar{n} = 0$ ) and the infinite temperature ( $\bar{n} \rightarrow \infty$ ) cases.

For the zero temperature case,  $\mathcal{L}_2^S = 0$ , and the only spontaneous decay term leads to a purely dissipative process. In the long-time limit, this process drives the corresponding qubit to its ground state  $|1\rangle$ , thus the GQDs disappear for arbitrary initial state. In Fig. 3, we showed the  $\gamma t$  dependence of the three GQDs for  $|\Psi\rangle$  with  $\alpha^2 = 0.5$  and  $\bar{n} = 0$ . For  $\mathcal{E}_{AB}$ , by comparing with Fig. 1(b), one can see that they exhibit very similar behaviors, except that the decay rates are obviously decreased, and the critical times for the SCs ( $\gamma t_c \simeq 0.485$  and  $0.609$ , respectively) are also slightly delayed. For  $\mathcal{E}_A$ , there is also single SC for both  $D_B(\rho)$  ( $\gamma t_c \simeq 0.693$ ) and  $D_H(\rho)$  ( $\gamma t_c \simeq 0.609$ ), which occurs earlier than those for the finite temperature reservoir (cf. Fig. 3(b) and Fig. 2(b)). Moreover, as showed by the blue line in Fig. 3(b), the HDD is increased with  $\gamma t$  during the region  $\gamma t \in [0.482, 0.609]$  (which is a reflection of the fact that the quantum discord can increase under the local operation on one party of the system [46]), while the TDD and the BDD are always decreased. This means that different discord measures may lead to different orderings of quantum states, and it confirmed again that what the discord reveals is in fact the combined result of the chosen discord and the quantum state other than a property of the state itself. Of course, the increase for HDD is slight and transient, and after  $\gamma t > 0.609$ , it decays to zero gradually. Finally, for  $\mathcal{E}_B$ , the three GQDs still show qualitatively the same  $\gamma t$  dependence with those for the finite temperature reservoirs, with however the decay rates are evidently decreased.

For the infinite temperature case, we have  $\mathcal{L}_1^S = \mathcal{L}_2^S$ , the decay and excitation processes occur at exactly the same rate, and the noise induced by the transitions between the two levels brings an arbitrary initial state into the maximally mixed one. For concise of the paper, we do not present the plots here. But the numerical results showed that for the initial state  $|\Psi\rangle$  with  $\alpha^2 = 0.5$ , all the three GQDs decay smoothly and monotonously with the increasing  $\gamma_0 t$  ( $\gamma_0 = \bar{n}\gamma$ ), and there are no SCs being observed for them.

Finally, as the SCs displayed in Figs. 1, 2, and 3 are obtained via numerical methods, one may wonder whether they are the real SCs or not, this is because sometimes it is possible that what one observes as a SC might be the result of a quick change that is actually not sudden when analyzed for smaller time intervals [30]. For the TDD, as its analytical expressions are given in Eqs. (13) and (14), it is evident that it does not experience SC for the model considered here. For the HDD and BDD, as the square root of the density operator  $\rho$  cannot be derived analytically, analytical solutions of  $D_H(\rho)$  and  $D_B(\rho)$  cannot be obtained. But the changes observed in the three figures are actually exactly sudden, and they are caused by the discontinuity of the optimal angle related to measurement op-

erators  $\{\Pi_k^A\}$ . In fact, by writing  $\Pi_{1,2}^A = (I_A \pm \vec{u} \cdot \vec{\sigma})/2$ , and the unit vector  $\vec{u} = (\sin \theta \cos \phi, \sin \theta \sin \phi, \cos \theta)$ , we found that for the considered state in this paper, both  $D_H(\rho)$  and  $D_B(\rho)$  are independent of the angle  $\phi$ , but for the case of the single SC, the optimal  $\theta$  for both  $D_H(\rho)$  and  $D_B(\rho)$  is given by  $\pi/4$  before the SC point, and it changes abruptly to  $\pi/2$  after the SC point. Moreover, for the case of double SCs, the optimal  $\theta$  changes abruptly from  $\pi/2$  to  $\pi/4$  and then back to  $\pi/2$  at the SC points. All these correspond to SCs of the optimal  $\{\Pi_k^A\}$ , and therefore the changes observed for both  $D_H(\rho)$  and  $D_B(\rho)$  are actually sudden.

## V. SUMMARY

In summary, we have investigated time evolution and the accompanying singular behaviors of the TDD, BDD, and HDD. To focus exclusively on the singular behaviors of them as caused solely by the thermal reservoir, the two qubits of the central system are assumed to be spatially separated far away from each other, and thus there are no direct interactions between them, that is, every qubit interacts with its own independent reservoir.

By solving analytically the master equation describing the evolution of the two qubits, we analyzed dynamics of the three GQDs, and found that they are incompatible in characterizing quantum correlations, although they are all well defined from a geometric perspective. Our findings are illustrated through two distinct behaviors of the three GQDs. First, we found that the three GQDs may exhibit completely different SCs for both the two-sided and the one-sided reservoirs. The critical times for the SCs and the times of SCs are strongly dependent on the choice of the GQD measure and the form of the initial state. Different GQD measures have different SCs, and thus the SCs are in fact the combined result of the chosen GQD measure and the quantum state, but not the intrinsic property of a state itself. This is fundamentally different from the sudden death of entanglement, which is independent of the entanglement measure. Moreover, we also revealed the relativity of different GQDs. To be explicit, we found that the thermal reservoir may lead to a generation of quantum states manifesting different orderings, and this implies that different GQDs are incomparable as their behaviors may not only be quantitatively but also be qualitatively different.

## ACKNOWLEDGMENTS

This work was supported by NSFC (11205121), and NSF of Shaanxi Province (2014JM1008).

- 
- [1] M.A. Nielsen, I.L. Chuang, Quantum Computation and Quantum Information, Cambridge University Press, Cambridge, 2000.
  - [2] L. Amico, R. Fazio, A. Osterloh, V. Vedral, Rev. Mod. Phys. 80

(2008) 517;

R. Horodecki, P. Horodecki, M. Horodecki, K. Horodecki, Rev. Mod. Phys. 81 (2009) 865.

- [3] K. Modi, A. Brodutch, H. Cable, T. Paterek, V. Vedral, Rev.

- Mod. Phys. 84 (2012) 1655.
- [4] A.K. Ekert, Phys. Rev. Lett. 67 (1991) 661.
  - [5] D.P. DiVincenzo, D. Eacon, J. Kempe, G. Burkard, K.B. Whaley, Nature 408 (2000) 339.
  - [6] J.W. Pan, Z.B. Chen, C.Y. Lu, H. Weinfurter, A. Zeilinger, M. Żukowski, Rev. Mod. Phys. 84 (2012) 777.
  - [7] H. Ollivier, W.H. Zurek, Phys. Rev. Lett. 88 (2001) 017901; L. Henderson, V. Vedral, J. Phys. A 34 (2001) 6899.
  - [8] A. Datta, A. Shaji, C.M. Caves, Phys. Rev. Lett. 100 (2008) 050502.
  - [9] B. Dakić, et al., Nat. Phys. 8 (2012) 666.
  - [10] A. Datta, S. Gharibian, Phys. Rev. A 79 (2009) 042325.
  - [11] S. Wu, U.V. Poulsen, K. Mølmer, Phys. Rev. A 80 (2009) 032319.
  - [12] M. Piani, P. Horodecki, R. Horodecki, Phys. Rev. Lett. 100 (2008) 090502; M. Piani, M. Christandl, C.E. Mora, P. Horodecki, Phys. Rev. Lett. 102 (2009) 250503.
  - [13] V. Madhok, A. Datta, Phys. Rev. A 83 (2011) 032323.
  - [14] D. Cavalcanti, L. Aolita, S. Boixo, K. Modi, M. Piani, A. Winter, Phys. Rev. A 83 (2011) 032324.
  - [15] M. Gu, et al., Nat. Phys. 8 (2012) 671.
  - [16] A. Streltsov, H. Kampermann, D. Bruß, Phys. Rev. Lett. 106 (2011) 160401; M. Piani, S. Gharibian, G. Adesso, J. Calsamiglia, P. Horodecki, A. Winter, Phys. Rev. Lett. 106 (2011) 220403; M.F. Cornelio, M.C. de Oliveira, F.F. Fanchini, Phys. Rev. Lett. 107 (2011) 020502.
  - [17] M. Piani, Phys. Rev. A 86 (2012) 034101; X. Hu, H. Fan, D.L. Zhou, W.M. Liu, Phys. Rev. A 87 (2013) 032340.
  - [18] T. Werlang, S. Souza, F.F. Fanchini, C.J. Villas Boas, Phys. Rev. A 80 (2009) 024103.
  - [19] B. Wang, Z.Y. Xu, Z.Q. Chen, M. Feng, Phys. Rev. A 81 (2010) 014101.
  - [20] M.L. Hu, H. Fan, Ann. Phys. 327 (2012) 851.
  - [21] L. Mazzola, J. Piilo, S. Maniscalco, Phys. Rev. Lett. 104 (2010) 200401.
  - [22] X.M. Lu, Z.J. Xi, Z. Sun, X.G. Wang, Quantum Inf. Comput. 10 (2010) 0994.
  - [23] J.S. Xu, X.Y. Xu, C.F. Li, C.J. Zhang, X.B. Zou, G.C. Guo, Nat. Commun. 1 (2010) 7.
  - [24] W. Song, Z.L. Cao, Int. J. Theor. Phys. 53 (2014) 519.
  - [25] T. Chanda, A.K. Pal, A. Biswas, A. Sen(De), U. Sen, arXiv:1409.2096.
  - [26] J. Maziero, L.C. Céleri, R.M. Serra, V. Vedral, Phys. Rev. A 80 (2009) 044102.
  - [27] F.F. Fanchini, T. Werlang, C.A. Brasil, L.G.E. Arruda, A.O. Caldeira, Phys. Rev. A 81 (2010) 052107.
  - [28] R. Auccaise, et al., Phys. Rev. Lett. 107 (2011) 140403.
  - [29] G. Karpát, Z. Gedik, Phys. Lett. A 375 (2011) 4166.
  - [30] J.P.G. Pinto, G. Karpát, F.F. Fanchini, Phys. Rev. A 88 (2013) 034304.
  - [31] C.S. Yu, B. Li, H. Fan, Quantum inf. comput. 14 (2013) 0454.
  - [32] L.X. Jia, B. Li, R.H. Yue, H. Fan, Int. J. Quantum Inf. 11 (2013) 1350048.
  - [33] T. Yu, J.H. Eberly, Phys. Rev. Lett. 97 (2006) 140403.
  - [34] F.M. Paula, T.R. de Oliveira, M.S. Sarandy, Phys. Rev. A 87 (2013) 064101.
  - [35] B. Aaronson, R.L. Franco, G. Compagno, G. Adesso, New J. Phys. 15 (2013) 093022.
  - [36] J.D. Montealegre, F.M. Paula, A. Saguia, M.S. Sarandy, Phys. Rev. A 87 (2013) 042115.
  - [37] F. Ciccarello, T. Tufarelli, V. Giovannetti, New J. Phys. 16 (2014) 013038.
  - [38] L. Chang, S. Luo, Phys. Rev. A 87 (2013) 062303.
  - [39] D. Girolami, T. Tufarelli, G. Adesso, Phys. Rev. Lett. 110 (2013) 240402.
  - [40] D. Spehner, M. Orszag, New J. Phys. 15 (2013) 103001.
  - [41] B. Aaronson, R.L. Franco, G. Adesso, Phys. Rev. A 88 (2013) 012120.
  - [42] D. Spehner, M. Orszag, J. Phys. A 47 (2014) 035302.
  - [43] B. Dakić, V. Vedral, Č. Brukner, Phys. Rev. Lett. 105 (2010) 190502; S. Luo, S. Fu, Phys. Rev. A 82 (2010) 034302.
  - [44] H.-P. Breuer, F. Petruccione, The Theory of Open Quantum Systems, Oxford University Press, Oxford, 2001.
  - [45] B. Bellomo, R.L. Franco, G. Compagno, Phys. Rev. Lett. 99 (2007) 160502.
  - [46] A. Streltsov, H. Kampermann, D. Bruß, Phys. Rev. Lett. 107 (2011) 170502.